RSC Advances



This is an *Accepted Manuscript*, which has been through the Royal Society of Chemistry peer review process and has been accepted for publication.

Accepted Manuscripts are published online shortly after acceptance, before technical editing, formatting and proof reading. Using this free service, authors can make their results available to the community, in citable form, before we publish the edited article. This Accepted Manuscript will be replaced by the edited, formatted and paginated article as soon as this is available.

You can find more information about *Accepted Manuscripts* in the **Information for Authors**.

Please note that technical editing may introduce minor changes to the text and/or graphics, which may alter content. The journal's standard <u>Terms & Conditions</u> and the <u>Ethical guidelines</u> still apply. In no event shall the Royal Society of Chemistry be held responsible for any errors or omissions in this *Accepted Manuscript* or any consequences arising from the use of any information it contains.



Performance of palladium and platinum supported on alumina pillared clays in the catalytic combustion of propene

A. Aznárez, A. Gil*, S.A. Korili

Department of Applied Chemistry, Building Los Acebos, Public University of Navarra, Campus of Arrosadia, E-31006 Pamplona, Spain

Abstract

The effect that the metal content of various pillared-clay-supported catalysts may have on the oxidation of propene was studied in this work. For this purpose, an alumina pillared montmorillonite (Al-PILC) was used as a support for palladium and platinum. The catalysts, with metal loadings of between 0 and 2 wt.%, were characterized by chemical analysis, nitrogen physisorption at -196°C, carbon dioxide physisorption at 0°C, X-ray photoelectron spectroscopy (XPS), X-ray powder diffraction (XRD), CO and H₂ chemisorption at 35°C, NH₃ chemisorption at 70°C and temperature-programmed reduction (TPR). Bulk PdO, Pd, and palladium-alumina structures were detected for the palladium catalysts. Likewise, bulk PtO₂ and small PtO₂ particles, which partially interact with the support, were observed for the Pt/Al-PILC catalysts. The results obtained suggest that the propene oxidation over Pd/Al-PILC and Pt/Al-PILC is a structure sensitive reaction as the turnover frecuencies are affected by metal dispersion and the structure of the surface catalysts.

Keywords: Pillared clays; Palladium platinum supported catalysts; Propene/propylene combustion.

* Corresponding author:

E-mail address: andoni@unavarra.es. Tel.: + 34 948 169602. Fax: + 34 948 169602

1. Introduction

Volatile organic compounds (VOCs) are a group of primary atmospheric air pollutants that contribute to a wide number of direct, carcinogenic or mutagenic, and indirect effects, ozone and smog precursors, on health and the environment. Process modification, including the substitution of materials to reduce VOC input into the process, changes in operating conditions to minimize VOC formation or volatilization, and changes in equipment to reduce exhaust sources, is usually the preferred alternative when it comes to reducing VOC emission. However, VOC removal technologies, such as adsorption, absorption, condensation, and thermal and catalytic combustion, amongst others, may also be used in addition to, or instead of, process modifications. The choice of technology mainly depends on the nature of the VOC, its concentration, and the flow rate of the waste gas. Thus, thermal combustion to carbon dioxide and water is the most widely used technology for the abatement of VOCs, especially when these organics cannot be recycled. However, as this process must be performed at high temperatures, usually above 1000°C, it requires the use of additional fuel and temperature-resistant materials and generates by-products such as NO_x. As a result, catalytic combustion is often a better solution for the elimination of low concentrations of VOCs as it offers several environmental advantages compared to thermal combustion, including the ability to operate at lower temperatures and the formation of lower amounts of by-products. Noble metals and transition metal oxides are commonly used as catalysts for the combustion of VOCs. The former are well-known, high-performance oxidation catalysts that are widely used for controlling exhaust gas emissions such as VOCs, hydrocarbons, and CO.² In addition, as they are less liable to sulphur poisoning, they are preferred to metal oxides. Although palladium and platinum catalysts are most commonly used for complete oxidation reactions, other noble metals, such as ruthenium, osmium, iridium, silver, or gold, have also

been. However, the volatility of their oxides, reactivity with the supports, and activity mean that palladium and platinum are by far the most common.³

Although information concerning the activities of palladium and platinum catalysts varies in the literature, some concepts are widely accepted. Palladium catalysts are more active in methane and CO combustion, whereas their platinum counterparts are more active for the combustion of hydrocarbons containing more than one carbon atom. It is also accepted that structure-sensitivity should be expected when the surface reaction involves the cleavage of a C-C bond. Similarly, the activity is strongly influenced by the interaction between Pd and the support. The degree of Pd-oxidation depends on the palladium particle size, whereas for platinum the formation of dispersed or crystalline phases depends more on the support composition and on the method of preparation.

The synthesis of porous solids from clay materials with a controlled pore structure is of great interest because of the potential applications of these materials in catalysis, purification, and sorption-based processes. Pillared interlayered clays (PILCs) are one of the most attractive groups of porous solids due to their controllable pore dimensions, which can be varied by changing the type of silicate layers and the pillaring agents. Furthermore, the incorporation of an active phase has extended the field of application of PILCs to cover several environmental processes, including the destruction of hazardous gaseous pollutants by complete oxidation. The catalytic applications of PILCs are mainly related to the nature and distribution of the pillars and to their surface properties.

There is an increasing interest in controlling the presence in gaseous emissions related to its characteristics and properties. ^{16,17} The catalytic combustion of propene has been widely studied, and several catalytic systems based on noble metals as well as transition metal oxides have been proposed. However, very little attention has been paid to catalysts supported on pillared clays (PILCs) for the catalytic combustion of propene. ^{13,18}

The choice of the catalyst support is important because of the role that support materials play in improving the efficiency of the catalyst by providing large pores and surface areas for the dispersal of active particles. Noble metals deposited on conventional supports such as Al₂O₃, SiO₂, and TiO₂ have been studied for the combustion of propene. Pillared clays are also of interest due to their high surface area, interesting surface acidity, and thermal stability. Despite being value added materials from natural products and having very interesting properties, very little attention has been paid to transition metal oxide and noble metal catalysts supported on pillared clays for the catalytic combustion of propene. The advantage of using pillared clays with respect to other supports is that, starting from natural, inexpensive clays, it is possible to develop new materials with a microporous structure that can be controlled during the intercalation process, and create catalytic sites by incorporating metal cations. The catalyst design and the control of active site distribution are the two main reasons for choosing pillared clays as stable and selective catalysts in sustainable combustion reactions.¹⁵

The catalytic performance is influenced by many factors, such as the nature of the catalyst, metal particle size, metal loading, pre-treatment applied, presence of a promoter, and the reaction conditions. In the present work, which forms part of our systematic study of the preparation of metal catalysts supported on Al-PILCs, we have undertaken a study of the total oxidation of propene as a function of the following variables: the nature of the noble metal (Pd and Pt); the loading of the noble metal; the structure of the catalysts; and the effect of the pre-treatment. The novel aspects include the use of Pd/Al-PILC and Pt/Al-PILC catalysts in propene combustion, a comparison between these two series of catalysts, and a study of the sensitivity of propene combustion to the catalyst structure.

2. Experimental Section

2.1. Catalyst preparation

A montmorillonite from Tsukinuno, supplied by The Clay Science Society of Japan, was used as the starting material. The raw clay mineral is very pure, which allows a better identification by instrumental techniques. Chemical analysis gave the following composition: 59.83 wt.% SiO_2 , 20.66 wt.% Al_2O_3 , 3.41 wt.% Na_2O , 3.24 wt.% MgO, 2.40 wt.% Fe_2O_3 , 0.71 wt.% CaO, 0.15 wt.% TiO_2 and 0.15 wt.% K_2O . The XRD pattern revealed the presence of low amounts of quartz and caolinite. The specific surface area was found to be 9 m²/g and the total pore volume was 0.047 cm³/g. Its cationic exchange capacity (CEC) is 100 mequiv./100 g.

The montmorillonite was intercalated and pillared with alumina, according to a conventional pillaring procedure reported previously from our group, ¹⁹ where the aluminium polycation solution was prepared by slow addition of a 0.5 mol/dm³ solution of AlCl₃·6H₂O (Merck, p.a.) to a 1.5 mol/dm³ solution of NaOH under vigorous stirring, with an OH⁻/Al³⁺ molar ratio of 2. The hydrolyzed solution was allowed to age for 48 h at 50°C under continuous stirring. An Al/clay ratio of 10 mmol_{Al}/dm³·g_{clay} was used in the intercalation process. The clay powder was directly dispersed in the intercalating solution as this procedure decreases the amount of liquid used and the time required for completion of the process. The clay suspensions were kept in contact with the solution for 24 h at room temperature and then centrifuged and washed. The resulting intercalated clay was dried for 16 h in air at 50°C and then calcined for 4 h at 500°C in order to obtain the alumina-pillared clay. Supported metal catalysts were prepared by wet impregnation of the support with solutions of palladium (palladium(II) nitrate solution, 10 wt.% in 10 wt.% HNO₃, Sigma-Aldrich) and platinum salts ([Pt(NH₃)₂](NO₂)₂, Strem Chemicals). The metal salt/clay slurries were evaporated to dryness under reduced pressure in a rotary evaporator and the resulting solids dried at 120°C for 16 h before being calcined in air at 500°C for 4 h to form the final supported catalysts. The catalysts had metal loadings of 0.1, 0.5, 1 and 2 wt.%, and are referred to hereinafter as wt.Met, where wt. indicates the metal content and Met the metallic phase (Pd or Pt). The raw clay is referred to as Na-Mont, and the alumina pillared clay as Al-PILC. The catalytic series are referred to as Pd/Al-PILC and Pt/Al-PILC.

2.2. Catalyst characterization

The metal content was determined after extraction by acid digestion by inductively coupled plasma-optical emission spectroscopy (ICP-OES) using a Varian Vista-MPX instrument.

Gas adsorption experiments with nitrogen (Air Liquide, 99.999 %) at -196°C and carbon dioxide (Air Liquide, 99,998 %) at 0°C were performed using a static volumetric apparatus (Micromeritics ASAP 2010 adsorption analyser). All samples (0.2 g) were degassed for 24 h at 200°C at a pressure lower than 0.133 Pa.

X-ray photoelectron spectroscopy (XPS) analysis was performed using an SSI X-probe (SSX-100/206) spectrometer from Surface Science Instruments (USA). The analysis chamber was operated under ultrahigh vacuum with a pressure close to 5 · 10⁻⁷ Pa, and the sample was irradiated with monochromatic Al Kα (1486.6 eV) radiation (10 kV; 22 mA). For these measurements, the binding energy (BE) values were referred to the C-(C,H) contribution of the C 1s peak at 284.8 eV. Data treatment was performed using the CasaXPS program (Casa Software Ltd, UK). Molar fractions were calculated using peak areas normalised on the basis of acquisition parameters and sensitivity factors provided by the manufacturer. The C 1s, O 1s, Ca 2p, Mg 2s, Si 2p, Al 2p, Pd 3d, and Pt 4f peaks were used for the quantitative analysis. Based on the XPS analysis, the XPS surface ratio of a given element is defined as the atomic concentration of the element (%) with respect to the concentration of the major element of the support (Si) (%). A special procedure was applied to decompose and compare the poor signal-to-noise ratio for the Pd 3d spectra. Thus, the 0.1Pd 3d spectra were summed to create a composite spectrum, then the model shape of the Mg Auger lines, as obtained from Pd-free

spectra, were used to fit this composite spectrum together with doublet components related to the Pd. Finally, the obtained model decomposition, number of Pd doublet components with fixed binding energies and FWHM values, was applied to fit all the individual spectra to provide more comparable results.

The X-ray powder diffraction (XRD) patterns of non-oriented samples were obtained using a Siemens D-5000 diffractometer with Ni-filtered Cu K α radiation (40 kV and 30 mA).

Chemisorption of CO (Praxair, 99.99 %) and H₂ (Air Liquide, 99.999 %) was performed at 35°C using the static volumetric apparatus mentioned previously (Micromeritics ASAP 2010 adsorption analyzer). The samples (0.2 g) were pre-treated in flowing He (Praxair, 99.998 %) up to 350°C, then cooled to 100°C. At this temperature the samples were degassed under vacuum to a pressure of less than 5 µmHg. The samples were then reduced under a flow of pure H₂ at 360°C for 6 h and cooled to the adsorption temperature under flowing He. CO and H₂ adsorption data were collected in the pressure range 50-600 mmHg. After this first adsorption experiment, the samples were degassed for 0.5 h at 35°C and new adsorption data were collected in the same pressure range. The volumes of irreversibly adsorbed CO and H₂ were calculated from the difference between these two adsorptions.

The acidity of the catalysts was determined by adsorption of NH₃ (Air Liquide, >99.995 %) using a dynamic pulse method on a Micromeritics TPR/TPD 2900 instrument with 0.2 g of catalyst. The samples were pre-treated at a heating rate of 10°C/min, under a flow of 30 cm³/min of He (Praxair, 99.999 %), at 400°C for 3 h and then cooled to 70°C in the same stream. Ammonia pulses (0.5 cm³) were injected at 70°C until the area of consecutive eluted pulses was constant.

Temperature-programmed reduction (TPR) studies were performed using the same apparatus mentioned in the previous paragraph (Micromeritics TPR/TPD 2900 instrument). Firstly, the samples were pre-treated with N₂ (Air Liquide, 99.999 %) at 150°C for 90 min, at

a heating rate of 10°C/min, under a flow of 30 cm³/min. The TPR tests were carried out from room temperature up to 800°C, at a heating rate of 10 °C/min, under a total flow of 30 cm³/min (5 % H₂ in Ar, Praxair). Water and other possible compounds that might be formed during metal reduction and precursor decomposition were retained by a cold trap.

2.3. Catalytic performance

Propene combustion was carried out using an automated bench-scale catalytic unit (Microactivity Reference, PID Eng&Tech). The reactor was a tubular, fixed-bed, downflow type with an internal diameter of 0.9 cm. Catalyst samples were mixed with an inert material, at a weight ratio of 1:4, in order to dilute the catalyst bed and avoid hot spot formation. The propene concentration in the feed was 0.5% and the oxygen-to-hydrocarbon molar ratio was 20, with helium as the balance gas, up to a total feed flow of 150 cm³/min. The catalyst was stabilized for 120 min at each temperature to ensure steady-state conversion. Space velocities (GHSV), calculated at standard temperature and pressure and based on the total volume of the catalytic bed, were about 20,000 h⁻¹. Prior to the catalytic tests, one of the following pretreatments were applied to the catalysts: 1) in flowing air (100 cm³/min): heating to 150°C at 2°C/min, 2 h at 150°C and cooling to room temperature, or 2) in flowing H₂ (Air Liquide, 99.999%) (100 cm³/min): heating to 300°C at 2°C/min, 2h at 300°C and cooling to room temperature.

The reactants and the reaction product streams were analyzed online using an Agilent 6890 gas chromatograph system equipped with two detectors. Analysis of the permanent gases was performed by separating them into a two-column system consisting of an HP-PLOT Q and an HP-PLOT Molsieve 5A, in a series-bypass configuration, connected to a TCD. An HP-PLOT Alumina column connected to an FID was used for hydrocarbon analysis.

3. Results and discussion

3.1. Textural properties

From the nitrogen adsorption results of the catalysts, the isotherms are mainly of type I in the Brunauer, Deming, Deming and Teller (BDDT) classification.²⁰ The nitrogen capacity of adsorption at low relative pressures was the most important difference among the catalysts. From the textural properties of the palladium and platinum catalysts (see **Table S1**), together with the basal spacing (see section 3.3), the intercalation-pillaring processes were successful in all cases. The subsequent impregnation with the aqueous metal solutions resulted in a loss of surface area and pore volume in comparison with the initial support. A more detailed description of the micro- and mesoporous regions of the catalysts was obtained from the pore-size distributions (see **Figure S1**), which were calculated using the model proposed by Jaroniec-Gadkaree-Choma, and reviewed by Gil et al.¹² It can be seen from these distribution curves that a maximum occurs at 0.70 nm that has been related to the distance between the clay layers in previous works.¹²

A study of the surface and the porous network of the pillared clays can provide useful information regarding the location of the impregnated cations. The micropore volumes were calculated by means of the Dubinin-Radushkevich (DR) equation²¹ over the relative pressure range 0.01-0.034, indicating that all the catalysts present a similar CO₂ adsorption capacity (0.05 cm³/g, see **Table S1**). Gas adsorption measurements with nitrogen and carbon dioxide provide complementary characterization information for these materials.¹² While nitrogen adsorption characterizes the micropores between 0.5 and 2 nm, as well as pores up to 200 nm, carbon dioxide, as a result of its higher kinetic energy compared to nitrogen, characterizes micropores in the range 0.4-1.5 nm.²² According to the CO₂ measurements, the results presented in **Table S1** show that Al-PILC has the same micropore volume as all the metal-containing samples, thereby suggesting that pores with diameters of between 0.4 and 1.5 nm

are not influenced by the presence of metal species. The micropore volume obtained from the N_2 measurements differs among the samples, probably due to the presence of metal species in the micropore range characterized by N_2 , but not by CO_2 , that is, in micropores with diameters of between 1.5 and 2 nm.

The micropore surface is estimated by subtracting the external surface from the specific surface area. In Al-PILC, the micropore surface is 94% and the external surface is 6%. In comparison with the support properties, the external surface decreases more in the Pd/Al-PILC catalysts (7-23%) than in their Pt/Al-PILC counterparts (7-15%), except in the case of the 2Pt catalyst (31%), thus meaning that the proportion of particles situated on the external surface is greater for the palladium catalysts. In the case of the 2Pt catalyst, the platinum particles can block a significant portion of those micropores with diameters in the range 1.5-2 nm. The platinum particles therefore block the Al-PILC interlayers and are displayed on the external surface, thereby decreasing the external surface more than expected. The micropore surface decreases more in the Pt/Al-PILC catalysts (from 30 to 41% for 0.1 to 1Pt, and 67% in the case of the 2Pt catalyst) than in their Pd/Al-PILC counterparts (20-21%), thus meaning that the proportion of particles situated on the micropore surface is greater for the platinum catalysts. For the 2Pt catalyst, the micropore volume, or micropore surface, is halved on increasing the Pt loading from 0.1 to 2 wt.%.

3.2. X-ray photoelectron spectroscopy (XPS)

The binding energies (BEs), atomic ratios and composition of Al-PILC, Pt/Al-PILC and Pd/Al-PILC catalysts determined from XPS experiments are presented in **Tables 1 and 2**. Typical BEs in montmorillonite are 102.75 (Si 2p_{3/2}), 74.8 (Al 2p_{3/2}) and 532 eV (O 1s) (carbon C1s is used as reference).²³ The metal/Si atom ratio in the Pd/Al-PILC and Pt/Al-PILC series increases with Pd and Pt loading, meaning that both Pd and Pt phases are

preferentially deposited on the external surface of the clay. A comparison of the ratio between surface and bulk platinum (from chemical analyses, **Table S2**) gives the following order: 0.004 (2Pt) < 0.005 (1Pt) < 0.008 (0.5Pt) < 0.024 (0.1Pt). From these results, it can be concluded that the amount of Pt that is incorporated to the structure of the support during the synthesis step increases with Pt loading. In the case of the Pd/Al-PILC catalysts, the following order can be established: 0.026 (0.1Pd) < 0.031 (1Pd) < 0.035 (2Pd). The Pd/Si atomic ratio increases slightly with the increasing Pd loading, being concluded that the amount of Pd displayed on the external surface of the Al-PILC increases slightly with Pd loading.

The Pt $4f_{7/2}$ BEs for the Pt/Al-PILC catalysts (see **Table 1**) are in according with the corresponding reference values of 71.3^{24} and $74.1 \text{ eV}^{25,26}$ for Pt and PtO₂. Thus, two platinum phases can be distinguished in all the Pt/Al-PILC catalysts by measuring the Pt $4f_{7/2}$ XPS line. XPS analysis of Pt on Al-PILC is complicated by the fact that the Pt 4f lines (73-76 eV) overlap with the Al 2p lines (74 eV) and that Pt 4d lines (316-333 eV), which are weaker than Pt 4f lines, overlap with a magnesium auger line (305 eV). It was not possible to measure the Pt and PtO₂ fractions on the surface of the catalysts as a result of these interferences.

Three forms of palladium on the surface of all the samples were observed from the deconvolution of the XPS spectra of the Pd/Al-PILC catalysts into their individual components. The BEs measured for the Pd 3d_{5/2} line were 335.1, 336.5, and 338.1 eV. The BE at 335.1 eV is due to Pd, and that at 336.5 eV was attributed to bulk PdO. The peak at 338.1 eV was associated to PdO₂, or highly dispersed and deficiently coordinated (ionic) Pd²⁺ in intimate contact with the alumina support to form palladium-aluminate structures.²⁷⁻²⁹ According to the Lesage-Rosenberg model,³⁰ the anchoring of Pd atoms takes place in vacant octahedral aluminium sites to form species similar to an aluminate in which the metal atoms can be described as Pdⁿ⁺. These particles grow epitaxially with the support to form (111)

monocrystalline particles.³¹ The evidence obtained in this work from all the various characterization techniques is consistent with a metal-support interaction. Thus, the XPS results show that oxidized palladium exists in two distinct chemical states-bulk PdO and palladium-aluminate structures-at low surface concentrations. It should be noted that the percentage of the more interactive phase and the degree of oxidation of the palladium phase depend on the palladium loading (see **Table 2**). The following percentages were found for the more interactive phase in the Pd/Al-PILC catalysts: 0.1Pd (35%), 0.5Pd (18%), 1Pd (9%), and 2Pd (6%). Likewise, the following percentages were found for the degree of oxidation of the palladium phase: 0.1Pd (95%), 0.5Pd (92%), 1Pd (80%), and 2Pd (76%). It can therefore be concluded that the lower the palladium loading, and thus the smaller the palladium particles, the higher the percentage of the more interactive phase in the catalyst and the higher the degree of oxidation of the palladium phase.

3.3. X-ray diffraction (XRD)

The XRD patterns for the supported palladium and platinum catalysts are presented in **Figure S2** together with those for Al-PILC and the starting material (Na-Mont). The basal spacing d(001) of the pillared sample, as determined from the XRD pattern, was 1.64 nm and therefore clearly higher than the basal spacing of Na-Mont (1.20 nm). These results, together with the nitrogen adsorption results, are in accordance with the pillaring process.

The patterns for the samples prepared by wet impregnation reveal the presence of PdO and Pt. The diffraction peaks at 33.60, 33.90, 41.96, 54.84, 60.25 and 60.86° correspond to PdO (JCPDS file no. 06-0515), and those at 39.76, 46.24 and 67.45° correspond to Pt (JCPDS file no. 04-0802). No peaks corresponding to other metal species were detected for any of the catalysts. The PdO crystallite sizes, as estimated using the Scherrer equation with a main diffraction line for PdO at $2\theta = 33.9^{\circ}$, are 19.6 nm for 0.5Pd, 17.1 nm for 1Pd and 16.3 nm for

2Pd, thereby suggesting that PdO crystallite size decreases slightly with palladium content. As the two main diffraction lines for PdO, at $2\theta = 33.6$ and 33.9° , are included in the same peak for the sample, which in turn is located adjacent to a support peak, the peaks were deconvoluted in order to avoid a contribution of these factors to the crystallite size.

The Pt crystallite sizes, as estimated using the Scherrer equation³² with a main diffraction line for Pt at 2 θ = 33.76° are 9.9 nm for 0.5Pt, 10.3 nm for 1Pt and 13.1 nm for 2Pt, thus suggesting that Pt crystallite size increases with platinum content.

No reflections attributable to platinum oxides or metal Pd were observed in the diffraction profiles, thus suggesting that these forms of noble metals, if present in the catalysts, are in a very finely dispersed state.

3.4. Chemisorption of CO, H2 and NH3

The adsorption of CO and H_2 is presented in **Figure S3** for Al-PILC and two representative catalysts (1Pd and 1Pt). The total and reversible quantities of adsorbed CO and H_2 were obtained using the double isotherm method.³³ The difference between amounts adsorbed gives the irreversible part of chemisorbed gas, which is used to characterize the metal phases. Catalyst properties related to the metal phases are shown in **Table S2**. The metal dispersion, D(%), was calculated from the chemisorption results using the formula:

$$D(\%) = \frac{V_m \cdot M}{V_{mol} \cdot F \cdot \% Me} \cdot 100$$

where V_m is the irreversibly chemisorbed gas (cm³ STP per gram of catalyst), M is the molar mass of the metal (g per mol of metal), V_{mol} is the standard molar volume of the adsorbate (cm³ STP per mol), %Me is the mass fraction of metal and F is the stoichiometry factor (number of gas molecules per atom of metal) with the following values: CO/atom of metal =

1, and H₂/atom of metal = 0.5.^{32,34} In order to calculate the metal surface area per gram of catalyst, S_{Met} , cross-section areas per atom of metal of 0.0787 nm^2 for Pd and 0.0841 nm^2 for Pt were used.³² Assuming that the metallic particles on the surface of the catalysts are spherical and wholly exposed to adsorption, the mean surface particle size was calculated from the metal dispersion values using the equations dp_{Pd} (nm) = 112.1/D(%) and dp_{Pt} (nm) = 113.2/D(%), and densities for palladium and platinum of 12.02 and 21.45 g/cm³.³⁵

For the two series of catalysts, the general trend for CO and H₂ is a decrease in metal dispersion with an increase in metal loading. Palladium and platinum catalysts with very low metal loadings (0.1 and 0.5 Pd, and 0.1 Pt) did not chemisorb hydrogen (see **Table S2**). The suppression of hydrogen chemisorption indicates the possible existence of a strong metal-support interaction (SMSI) state.³⁶ Indeed, this has often been adopted as a simple test for such a state, which has been shown to occur in a number of systems comprising small metal particles, typically involving group VIII metals, dispersed on the surface of transition metal oxides whose surfaces can be reduced to form cations with lower valences. The changes in adsorptive, catalytic, and structural properties characteristic of the SMSI state strongly suggest an electronic interaction at the metal oxide interface.³⁷

In the case of 0.5Pt, although H_2 chemisorption was not totally suppressed, a higher chemisorbed volume of H_2 per gram of 0.5Pt would be expected. A comparison of the H_2 chemisorption results with those for CO chemisorption suggests that a higher dispersion, and thus a smaller particle size, would be expected.

Then, as the low load palladium catalysts are more affected by the SMSI effect than the platinum ones, it is concluded that the SMSI effect is more important in palladium-supported catalysts than in their platinum counterparts. The behavior of platinum can be explained by a high ratio between the Pt-Pt and oxidized platinum bond strengths, and thus weak interactions

with the support. In comparison with platinum, palladium-support interactions are stronger due to the higher affinity of palladium for oxygen.²⁸

It has been shown that there are slight differences in the particle sizes determined by XRD and gas chemisorption. These differences can be explained as being due to the phases measured and the aspects measured by these two techniques. Thus, since XRD provides information regarding the crystal structure of the bulk phase, gas chemisorption is a more sensitive technique for counting metal surface atoms as all surface atoms, irrespective of crystallite size, are probed at the molecular level. In other words, crystallite sizes based on XRD are volume-weighted average sizes whereas those based on gas chemisorption are surface-weighted average sizes. In the case of Pd/Al-PILC and Pt/Al-PILC catalysts, whereas XRD only provides the size of the bulk PdO and Pt phases, all surface atoms (the originally oxidized and reduced ones) are probed by gas chemisorption. Furthermore, a different trend in the particle sizes calculated using the two techniques is observed in the case of Pd/Al-PILC catalysts. Thus, whereas gas chemisorption suggests that particle size increases with increasing palladium loading, XRD suggests the opposite. This can be explained by the fact that, as shown by XPS, the lower the palladium loading in the catalyst, the more oxidized the palladium phase and therefore the greater the percentage of bulk PdO phase.

Interesting conclusions can be obtained comparing the metal particle sizes with the textural results presented in **Table S1** and the XPS conclusions presented in Section 3.2. Taking into account the results obtained from CO chemisorption, the dispersion decreases and the size of the metal particles increases with increasing metal content, especially in the case of Pd. Particle sizes in the ranges 3.8-24.9 and 3.8-8.8 nm were obtained for the palladium and platinum catalysts, respectively. In the case of Pd/Al-PILC catalysts, it should be noted that the large metal particles are mainly present on the external surface, in mesopores and on the sheets and edges of the clay, whereas in the case of Pt/Al-PILC catalysts, whose particles are

more dispersed and smaller than in palladium catalysts, these particles are located mainly in the porous structure of the support, in micropores with a pore diameter of between 1.5 and 2 nm and in mesopores. The Pt/Si atomic ratio obtained by XPS suggests that a significant number of platinum particles penetrate the clay interlayer for all Pt/Al-PILC catalysts. Thus, the decrease in the external surface for the Pt catalyst is mainly due to the location of the platinum particles mainly in the mesopores but not on the sheets and edges of the clay. In the case of 2Pt, the metallic phase is located in the mesopores plugging an important part of the bigger micropores. The proposed location of the metal phases is shown in **Scheme 1**.

Ammonia chemisorption provides an estimation of both Brönsted and Lewis acidity, and the amount of adsorbed ammonia is taken as a measure of the concentration of acid sites. The Brönsted acidity of montmorillonite essentially results from the dissociation of water molecules in the hydration shell of the interlayering exchangeable cations, whereas Lewis acidity results from the low coordination of aluminium atoms at the crystal edges of the clay sheet. It is widely accepted³⁸ that the Lewis acidity of Al-PILC is strongly related to the pillars, whereas a weak Brönsted acidity arises from the hydroxyl groups of the montmorillonite layers. Upon calcination, the pillars and silica layers of the clay induce the formation of stronger Lewis and new Brönsted sites.³⁹ The total acidity data, expressed as mmol of chemisorbed NH₃ per gram of sample, are given in **Table S2**. The acidity of Na-Mont increases strongly due to the pillaring process. The contribution of the pillars to the acidity of pillared clays is therefore likely to be mainly of the Lewis type. Except for 2Pt, the concentration of acid sites did not change significantly with respect to the support upon incorporation of palladium and platinum into the Al-PILC, thus indicating that the acidity is mainly due to Al-PILC. These slight differences in the concentration of acid sites are probably the net result of several factors, such as a change in the pH of the impregnation solution, the nature of the species adsorbed and their amount, the residual cations or protons present in the samples. In the case of the 2Pt catalyst, apart from the above-mentioned factors, the metal phase blocks a major part of the micropores and therefore of the pillars. As a result, the lower concentration of acid sites could be related to a decrease in the Lewis acidity provided by the pillars.

3.5. Temperature-Programmed Reduction (TPR)

The reducibility of the noble metal-supported catalysts was studied by temperature-programmed reduction (TPR, see **Figure 1**). The significant reduction process observed for the support at 640°C was related to the reduction of structural Fe³⁺ cations. As can be seen in Pd/Al-PILC and Pt/Al-PILC profiles, a shift in this peak to lower temperatures is observed as the metal loading increases.

The H₂-TPR profiles for the palladium catalysts are characterized by the presence of a negative peak at 70°C, which is related to the desorption of weakly adsorbed hydrogen from the Pd surface, and decomposition of the β-PdH phase formed at room temperature by diffusion of hydrogen into the Pd crystallites.⁴⁰ As can be seen, the higher the palladium loading, and thus the fraction of metallic palladium in the catalyst, the more pronounced the negative peak. The second region of H₂ consumption, which is observed between 100 and 200°C can be appreciated clearly only for 0.1Pd, is attributed to the reduction of small PdO species (oxide clusters). Another reduction process, which is observed in the temperature range 200-460°C, is attributed to the reduction of PdO particles interacting strongly with the surface of the support.²⁸ PdO is known to be easily reducible, even at room temperature. However, although our TPR analysis started at room temperature, reduction of the PdO aggregates was not observed.

Three hydrogen consumption peaks can be identified for the platinum catalysts. Two peaks centred at around 90 and 180°C can be observed in the first region, in which hydrogen

consumption occurs from room temperature up to 230°C. The TPR spectra also revealed a second H_2 consumption region at around 230-460°C. Huizinga et al. ⁴¹ have studied the influence of calcination temperature on the TPR profiles of Pt/Al_2O_3 samples prepared from $Pt(NH_3)_4(OH)_2$. Isolated Pt^{2+} ions were originally present in the dried but uncalcined sample. These authors detected the formation of Pt^{4+} species, probably small oxide particles, after calcination at several temperatures (200, 300 and 400°C), and after calcination at 500°C they detected the formation of PtO_2 particles. Thus, the platinum oxides proved easier to reduce upon increasing the calcination temperature. The oxidised platinum forms were reduced in the following order: PtO_2 particles (60-100°C) < Pt^{4+} species (small PtO_2 particles) (150-200°C) < isolated Pt^{2+} ions (240°C). Lieske et al. ⁴² investigated the effect of the precursor salt in Pt/Al_2O_3 catalysts by reducing samples at 500°C for 1 h, then re-oxidising and studying them by TPR in situ. The use of a non-chlorinated precursor and oxidation at between 200 and 500°C led to the formation of α -[PtO_2]_s, whose TPR peak appeared at temperatures close to 100°C.

In our case, the two peaks at lower temperatures could correspond to the reduction of PtO₂ particles (90°C) and smaller PtO₂ particles (190°C), whereas the peak at higher temperature can be assigned to platinum oxide interacting strongly with the surface of the support. It can therefore be concluded that the platinum-support interaction is influenced by several factors, including the calcination temperature, the nature of the support, and the nature of the metallic phase precursor.

The results for the platinum catalysts show that, besides the metallic Pt detected by XRD, bulk PtO₂ and small PtO₂ particles, which partially interact with the support, can be detected by XPS and TPR. For the palladium catalyst, although the XRD technique only showed diffraction peaks for bulk PdO, palladium-alumina structures and Pd species could also be detected by XPS and TPR. It should also be noted that the identification of PtO₂ and

Pd species, which are present in much lower percentages than metal Pt or bulk PdO, was not possible by XRD. It can therefore be concluded that the sensitivity of the XRD technique in the case of supported catalysts does not allow similarly solid conclusions to those obtained for unsupported phases to be obtained as the supported phase represents only a relatively small fraction of the solid investigated.

As we have seen from our characterization studies, platinum is mainly present as Pt whereas palladium is mainly in an oxidized state. As a result of its higher ionization potential than Pd (870 vs. 804.4 kJ/mol), Pt shows a higher tendency to be in the metal state. In contrast, the lower ionization potential of Pd means that it tends to be present in a higher oxidation state.

3.6. Catalytic performance

All samples were heated to the reaction temperature at a rate of 4°C/min in the presence of the reaction mixture, then stabilized for 120 min. Care was taken to ensure that the temperature remained stable and constant during the reaction at all the temperatures studied. As expected, the main reaction products were carbon dioxide and water, along with very small quantities of partial oxidation products, CO, depending on the sample and the temperature. The catalytic conversion was calculated in terms of the consumption of propene and the formation of CO₂, and the values obtained compared. Although they were generally in good accord, slight differences were observed in some cases, especially at low temperatures, where a slightly higher conversion was obtained from the propene consumption calculation. The observed effect results from the formation of small quantities of incomplete combustion species, such as CO. As the reaction is kinetically limited at low temperatures, the conversion depends on the interaction between hydrocarbon and oxygen molecules on the catalyst's surface. As the temperature increases, and the ignition region is reached, the reaction rate increases abruptly

due to the contribution of the reaction heat, see **Figure 2**. At higher temperatures, when conversion is complete, there are no products of incomplete combustion. Carbon mass balances of around 95-100% were obtained.

Yao⁴³ has studied the complete oxidation of propene over palladium, platinum and rhodium supported on γ-Al₂O₃. The rate and stoichiometric measurements were performed under oxygen-rich conditions in almost all cases. These authors found that the oxidation of propene was nonstoichiometric in some cases, with partial oxidation products (CO, aldehydes, etc.) being formed. As would be expected, the degree of deviation from stoichiometry for oxidation to CO₂ decreased with increasing O₂/olefin ratio and reaction temperature. Cant et al.⁴⁴ have also studied the catalytic oxidation of propene over silicasupported Pt, Pd, Ir, Ru, and Rh. In this case, although CO₂ and H₂O were the main reaction products, a wide variety of partial oxidation products were also formed in detectable amounts. Palladium produced small amounts of acrolein, acetone, and acetic acid, whereas only trace quantities of these compounds were formed over platinum. Acetaldehyde, C₃ acids and CO were also detected in trace amounts with palladium and platinum catalysts. In contrast to the above-mentioned works, many other studies dealing with the combustion of propene over palladium and platinum on various supports did not report the formation of partial oxidation products.⁴⁵⁻⁴⁹

As far as the mechanism of propene combustion over noble metal catalysts is concerned, Diehl et al.⁶ have proposed that, at low temperature or under oxygen-poor atmospheres, the first and most important step is propene adsorption to the surface via π -bonding between the C=C bond of the hydrocarbon and the metal atoms. The second step is transformation of this π -coordinated alkene-metal species into a di- σ species, which leads to cleavage of the C-C bond and reaction with the adsorbed oxygen. The most important step at high temperature is oxygen adsorption. Yao⁴³ has reported that the rate of complete olefin

oxidation over Pd and Pt is strongly dependent on the O_2 partial pressure and that the reaction is inhibited by hydrocarbons (negative orders) as a result of strong adsorption of the unsaturated hydrocarbon to the Pt and Pd surface via π -bonds. The oxidation rate at high olefin/ O_2 ratios or low temperatures, where a non-stoichiometry exists, is further suppressed by strong adsorption of the partial oxidation products. At lower olefin/ O_2 ratios or higher temperatures, the rate is enhanced by removal of the products from the surface sites by O_2 . The double bond plays a key role in the oxidation reaction, with its adsorption and cleavage being the rate-controlling step. In light of this, the differences observed in this study between the catalytic performance of the palladium and platinum catalysts could be related to the reactivities of adsorbed propene and oxygen on the metal surfaces. Likewise, the lower efficiency of the platinum catalysts compared to their palladium counterparts could be due to a higher degree of propene adsorption on platinum than on palladium. Thus, the noble metal oxides in contact with the mixture feed are reduced at low temperatures because of the strong adsorption of propene (reductant molecule) on palladium and platinum by π -bonding. As a result, oxidation of propene occurs on the reduced palladium and platinum surface.

The turnover frequency (TOF) is a measure of the rate of reaction with respect to the number of catalytic sites and is defined as the number of catalytic cycles per unit time (generally per second). As the number and nature of the active sites are difficult to identify, it is usually assumed that each surface atom is an active site. A calculation of the percentage of metal exposed, as measured by chemisorption on the supported catalysts (see Section 3.4.), makes it straightforward to calculate the nominal TOF. We considered the metal dispersion measured by CO chemisorption, and the palladium and platinum sites were only measured for the fresh catalysts, that is, before catalytic pre-treatment and rate measurements.

As the complete oxidation of propene is a highly exothermic reaction (~1900 kJ/mol), the parasitic effect of heat and mass transfer, especially inside the pores of high specific area

materials, is a major obstacle to the correct measurement of intrinsic kinetic data in heterogeneous catalysis. Since heat/mass transport limitations may affect the measured rates by a factor of 1-10,000, they must be avoided when measuring TOF data. As a result, the Koros-Nowak test, which involves performing the reaction for at least two catalysts with different metal loadings but similar metal dispersion percentages, was employed to check for the absence of heat- and mass-transfer limitations. The results are summarized in **Table 3**. As practically the same TOF value was obtained for the Pd/Al-PILC (1 and 2Pd) and Pt/Al-PILC (0.5 and 1Pt) catalysts, it can be concluded that our data are not affected by heat or mass transfer.⁵¹

In the kinetic expression, TOF(1/s) can be described as:

$$\ln(TOF) = \ln(A) - \frac{E_a}{R} \cdot \frac{1}{T}$$

where A is the pre-exponential factor (1/s), E_a the activation energy (J/mol), R the universal gas constant (J/K mol) and T the temperature (K). In order to evaluate the kinetic parameters, the reactor was operated isothermally and the conversion was limited to less than 15% to ensure differential reactor conditions. The performance of the catalysts at various temperatures is evaluated from an Arrhenius plot, from which activation energies were calculated. At a lower temperature the chemical reaction is slow and thereby rate controlling. In this region, the slope of the curve is proportional to the intrinsic activation energy (E_a). Thus, the activation energies and pre-exponential factors reported in **Table 4** have been obtained using only data in the kinetic region.

3.6.1. Pre-treatment in flowing air. The catalytic conversion of the support is improved even by those catalysts with a metal loading of 0.1 wt.% (see Figure 2). The nominal TOFs on catalysts with a metal (Pd, Pt) loading of between 0.5 and 2 wt.% are similar, and higher than those on the 0.1 wt.% -loaded catalysts in the entire temperature range. Also, for a given temperature, the nominal TOFs for the Pd/Al-PILC catalysts are higher than for their Pt/Al-PILC counterparts. Thus, the Pd/Al-PILC catalysts are more active than the Pt/Al-PILC ones in propene combustion. A similar trend was observed by Yao⁴³ for the catalytic oxidation of propene over Pd/ γ -Al₂O₃ and Pt/ γ -Al₂O₃. The specific activity for propene oxidation was higher with palladium catalysts, which in turn gave higher degree of complete consumption to CO₂ and H₂O, than with platinum ones. In contrast Cant et al., ⁴³ who studied the catalytic oxidation of propene over Pd/SiO₂ and Pt/SiO₂, found that platinum catalysts were more selective for CO₂ than palladium ones and were also more active.

However, the most conventional way of comparing activities is by studying the TOFs at a given temperature at which, as pointed out before, differencial reactor conditions must be ensured. Treatment of the Pd/Al-PILC and Pt/Al-PILC catalysts in flowing air resulted in the complete combustion of propene being sensitive to crystallite size (see **Table 4**). For Pd/Al-PILC catalysts the TOF ranged from 0.03 to 0.25 when the particle size was varied between 3.8 and 24.9 nm. Indeed, the nominal TOF decreased with an increase in the percentage of the more interactive palladium oxide in these catalysts. Note that the measured values for the apparent activation energies vary within a broad range. For the Pt/Al-PILC catalysts, there is a particle size for which the nominal TOF is maximized. Specifically, the nominal TOF increases with particle size from 0.1 to 0.5Pt. It has been observed that the nominal TOF is almost constant over a wide ride of particle sizes for both series (1 and 2Pd, as well as 0.5, 1 and 2Pt). As a result, the nominal TOF for the Pd/Al-PILC catalysts is maximized in the particle size range 20-24.9 nm, whereas for the Pt/Al-PILC catalysts it is maximized in the

particle size range 6-8.8 nm. Thus, propene oxidation over the Pd/Al-PILC and Pt/Al-PILC catalysts is a structure-sensitive reaction as the TOF is affected by Pd and Pt dispersion and the structure of the surface of the catalysts. A decrease in metal loading leads to a decrease in particle size, an increase in the percentage of more interactive oxides, and a decrease in the nominal TOF.

The results obtained in this study suggest that the nature of the metal, the dispersion of the metallic phases, the support and thus the percentage of the more interactive oxide (surface morphology) are the main factors governing the oxidation of propene on these catalysts.

As it has been concluded that the active phase in propene combustion is metallic palladium, it is also possible to compare the real TOF for the Pd/Al-PILC catalysts using the XPS results. In this way the number of active sites is quantified using the dispersion of the metallic phase and the metallic palladium surface composition. The fact that the nominal TOF was severely underestimated in comparison to the real TOF, corroborates the sensitivity of the reaction of the Pd/Al-PILC catalysts' structure. The trend for both values is the same, the TOF increases with particle size from 0.1 to 0.5Pd and then remains constant over a wide range of particles sizes (0.5, 1, and 2Pd catalysts). The real TOF for the Pt/Al-PILC catalyst could not be calculated as it was not possible to quantify the percentage of platinum oxides on the catalytic surface. However, bearing in mind that the active site in the studied reaction is metallic platinum and that this is also the predominant phase in the fresh catalysts, it is clear that the difference between the nominal and real TOFs should not be large.

The activation energies, pre-exponential factors, and TOFs, calculated at low temperature, are shown in **Table 4**. In the case of the Pd/Al-PILC catalysts, the activation energies correlate inversely with the catalytic performance. In other words, and although this is not intuitive, the Pd catalyst with the highest activation energie (2Pd) is the most active.

There is also a tendency for high activation energies to be accompanied by high preexponential factors.

This can be explained by the compensation effect, or enthalpy-entropy compensation. Thus, an increase in the pre-exponential factor with increasing activation energy suggests some sort of compensation for a loss of freedom in the transition state as a result of a reduced enthalpy for the transition state while the free energy remains constant. As the pre-exponential factor of the activated complex increases, the catalytic reaction becomes closer to the homogeneous one and the bonding of the activated complex to the active site becomes weaker. ^{50,52}

The lower activation energies for the platinum catalysts (23.4-159 kJ/mol) than for their palladium counterparts (212-255.2 kJ/mol) suggest that less energy is needed to activate the reaction in the case of platinum catalysts. However, the activation energies for the palladium and platinum catalysts correlate inversely with catalytic performance, and the catalysts with the highest activation energies (Pd/Al-PILC) are the most active. In the case of the Pt/Al-PILC catalysts the compensation effect does not exist.

We suppose that this difference is related to the oxidation state of the palladium and platinum phases. After pre-treatment in air, the palladium and platinum oxides in contact with the feed mixture begin to be reduced as the catalytic reaction starts. Thus, the activation energy for the Pd/Al-PILC catalysts would be the sum of the activation energy for propene combustion and for reduction of the highly oxidized palladium phase. In contrast, as the main state for the Pt/Al-PILC catalysts is metallic (except for 0.1Pt which is more oxidized), which in turn is the active phase, the activation energy would mainly include the activation energy for propene combustion.

3.6.2. Pre-treatment in flowing hydrogen and comparison between the two pretreatments. After the pre-treatment at 300°C in flowing hydrogen, the nominal TOF for the 0.1 wt.% -loaded catalysts is higher than that for the catalysts with a metal loading of between 0.5 and 2 wt.% up to 200°C in the case of palladium catalysts, and up to 400°C in the case of the platinum ones. Thus, these results show that, in comparison with pre-treatment in air, reduction in H₂ before reaction has a positive effect on the rate of the lower loaded catalysts, mainly in the case of the 0.1 wt.% -loaded ones. Pre-treatment with H₂ improves, in comparison with the pre-treatment in air, the rate of C₃H₆ oxidation of the 0.1Pd catalyst in the entire temperature range. However, for the 1Pd catalyst, the rate is improved only up to 200°C. In the case of the Pt/Al-PILC catalysts, it is clear that the reduction in H₂ improves the rate of C₃H₆ oxidation to a lesser extent than in the case of the Pd/Al-PILC catalyst. For the 0.1Pt catalyst, the rate is improved up to 350°C, whereas no improvement has been observed for the 1Pt catalyst. Thus, by pre-treating the Pd/Al-PILC and Pt/Al-PILC catalysts in H₂, the rate of C₃H₆ oxidation is improved to a higher extent for the Pd/Al-PILC catalysts than for the Pt/Al-PILC ones. Moreover, this improvement is greater for the low-loaded catalysts than for the high-loaded ones. Finally, the positive effect on the rate of reaction is greater at low temperatures, and decreases as the temperature is increased. In line with these results, are those obtained from a comparison of the nominal TOF at 195°C after the two pre-treatments. For the Pd/Al-PILC catalysts, the ratio (TOF H₂/TOF Air) follows the order 0.1Pd (10.3) > 0.5Pd~(2.4) > 1Pd~(1.6) > 2Pd~(1.1). Similarly, the ratio (TOF H₂/TOF Air) for the Pt/Al-PILC catalysts follows the order 0.5Pt(1.5) > 1Pt(1.2) > 2Pt(1.0). The difference between both pre-treatments, although slight for most of catalysts, is greater for the palladium catalysts than the platinum ones, and also greater for the 0.1 wt.% -loaded catalysts than the 2 wt.% loaded ones.

A marked decrease in the activation energies is observed for the Pd/Al-PILC catalysts pre-treated with hydrogen in comparison with those pre-treated in flowing air (see **Table 4**). As the active site for this reaction is metallic palladium, this effect is likely to be related to reduction of the big percentage of palladium oxides during the hydrogen pre-treatment. Pre-treatment of the 0.1Pt catalyst with hydrogen also resulted in a marked decrease in the activation energies, whereas for 0.5, 1 and 2Pt basically no change was observed. This means that the 0.1Pt catalyst also has an important percentage of platinum oxides, whereas the percentage of these in the 0.5, 1 and 2Pt catalysts is considerably smaller.

Pre-treatment of the catalysts in H₂ before reaction result in an important reduction of the oxides, and thus in a change of the surface morphology of the catalysts, regarding when pre-treated in air. Under these conditions, the nominal turnover rates increase. Under steady-state conditions, it is concluded that the oxidation of propene over the Pd/Al-PILC and Pt/Al-PILC catalysts is a *structure sensitive* reaction, as TOF changes with particle size and surface morphology.

3.6.3. Characterization of the catalysts after the reaction. The state of palladium after the reaction (catalysts pre-treated in flowing air) has been studied by means of TPR and XRD. A comparison of the TPR patterns for the catalysts used for the total oxidation of propene with those for the catalysts previously reduced in hydrogen at 300°C for 2 h and freshly prepared ones can be found in **Figure 3**. These findings confirm the difference between the catalysts used for the combustion of propene and those almost totally reduced in hydrogen at 300°C for 2 h. Thus, the pattern of the used samples is intermediate between those for the fresh and the reduced catalysts, thereby suggesting that the palladium oxides in the former have been partially reduced. The negative peak at 70°C, which is related to the presence of metallic palladium, is not observed for the 2Pd catalyst. The XRD patterns of this

catalyst (fresh and after use for propene combustion) were also studied (see **Figure 4**). Propene oxidation results in the appearance of very intense peaks at 39, 45.3, and 66.2°, which do not correspond to the characteristic diffraction peaks of the Pd phase. In light of these results, we can conclude that a new phase is formed due to the reaction. This new phase, referred to as PdX, was therefore compared with Pd. Taking the Pd phase (JCPDS file no. 046-1043), which contains diffraction peaks centered at 40.12, 46.66, and 68.12° as reference, it can be seen that the peaks for the new phase are displaced to slightly lower values. These findings confirm the differences between the lattice parameters of the Pd and PdX phases.

Ferhat-Hamida et al.⁵³ have studied the catalytic combustion of several hydrocarbons (propene, but-1-ene, and acetylene) over a 1 wt.% Pd/γ-Al₂O₃ catalyst prepared by impregnation of the support with a solution of palladium acetylacetonate in acetone. The hydrocarbon concentration was 0.4%, and the O₂ concentration was adjusted to change the stoichiometry. To investigate the effect of the oxygen/propene ratio on the chemical state of palladium, these authors studied various ratios, namely an absence of oxygen and a sub- and super-stoichiometric ratio. The significant transformation of palladium observed after propene oxidation was identified by means of XRD and TEM. The new palladium phase PdX, which exhibited a cubic structure with a higher lattice parameter than in Pd, was formed after both olefin and acetylene oxidation, although the PdX peaks recorded after acetylene oxidation were only about half the area of the corresponding peaks after alkene oxidation. The XRD spectra clearly showed the presence of the PdX phase (peaks at 39.1, 45.4, 66.3, and 79.6°), which was formed over a wide range of oxygen to olefin ratios but to a greater extent under oxygen rich conditions. The new palladium phase was hardly formed in the absence of oxygen in the reactant flow mixture. These authors concluded that O species should intervene in the construction of this new phase. Similarly, they concluded that the insertion of oxygen atoms into the fcc lattice of palladium induced an increase in the lattice parameter of Pd. In a

related study, Maillet et al.⁵⁴ concluded that the lattice parameter of the new phase was equal to 3.99 ± 0.003 Å, slightly greater than that of Pd (3.8898 Å). They proposed the formula PdO_{ξ} ($\xi \approx$ zero) for this new structure, with some oxygen remaining inserted in the Pd lattice. Thus, when palladium catalysts are pretreated in air, propene combustion occurs in a reduced palladium surface (PdX). While oxygen was weakly adsorbed on Pd, and not dissociated, the reductant molecule (C₃H₆) was strongly adsorbed by π -bonding on metals.

3.6.4. Stability of the catalysts in the reaction. Finally, the stability of the catalysts in the reaction was tested by reusing the catalysts in consecutive oxidation cycles and by performing long catalytic runs at constant oxidation temperatures. The evolution of propene conversion with time-on-stream at various temperatures for a selected number of catalysts is presented in **Figure S4**. The catalysts maintain their catalytic activity well after 30 h of reaction. Catalysts 0.1Pd and 2Pd were submitted to successive oxidation cycles (see **Figure 5**) and were pre-treated in flowing air before the first cycle, and after the first and second cycles. In this case, the catalysts also maintained their catalytic activity well after the three oxidation cycles, and practically no beneficial effect on their activity was observed after the re-oxidation cycles. Marécot et al.⁴⁸ obtained similar results in their study of the effect of successive oxidation cycles on the light-off temperatures of Pt/γ-Al₂O₃ catalysts for propene oxidation. Thus, whereas the light-off temperatures for chloride-containing platinum samples decreased to constant values after several oxidation cycles, no beneficial effect was observed for catalysts prepared from a dinitrodiammine precursor.

4. Summary and conclusions

An alumina-pillared clay has been used as a support for palladium and platinum catalysts, with various metal loadings, for the total oxidation of propene. Dispersed metallic phases with

particle sizes in the ranges 3.8-24.9 and 3.8-8.8 nm were obtained for the palladium and platinum catalysts, respectively. The larger palladium particles are mainly present on the external surface, in mesopores and on the sheets and edges of the clay, whereas the smaller platinum particles are located in the porous structure of the support, in micropores with pore diameters in the range 1.5-2 nm, and in mesopores. The characterization techniques employed have allowed bulk PdO, Pd, and palladium-alumina structures to be detected in the case of the Pd/Al-PILC catalysts. Bulk PtO₂, and small PtO₂ particles, partially in interaction with the support, were observed for the Pt/Al-PILC catalysts. The fraction of oxidized phase is much lower in platinum catalysts than in palladium ones. Thus, platinum is mainly present as Pt whereas palladium is mainly in an oxidized state.

The oxidation of propene over the Pd/Al-PILC and Pt/Al-PILC catalysts is carried out on the reduced palladium and platinum surface. The Pd/Al-PILC catalysts are more active than their Pt/Al-PILC counterparts, existing a direct relation between the selectivity for CO₂ and catalytic performance. Pre-treatment of the catalysts in H₂ result in an important reduction of the metal oxides, and thus in a change of the surface morphology of the catalysts. In these conditions, the nominal turnover frequencies are improved, being is higher for the Pd/Al-PILC catalysts than for the Pt/Al-PILC ones, for the low-loaded catalysts than for the high-loaded ones, and at low temperatures than at high ones. Under steady-state conditions, it is concluded that the oxidation of propene over Pd and Pt catalysts is a *structure sensitive* reaction, as TOF changes with particle size and surface morphology.

The treatment of palladium catalysts, pretreated in flowing air, with a propene/oxygen mixture leads to an incomplete PdO/Pd transformation phase. The structure obtained is close to that of metallic Pd, that is, a cubic phase, but with a slightly higher lattice parameter (3.99 instead of 3.89 Å). This difference could be the result of the presence of oxygen ions in the cubic face centered structure of metallic Pd.

The catalysts studies maintain their catalytic activity well after being submitted to successive oxidation cycles and after performing long catalytic runs at constant oxidation temperatures.

Acknowledgements

This work was funded by the Spanish Ministry of Science and Innovation (*MICINN*) and the European Regional Development Fund (*FEDER*) (project MAT2007-66439-C02). The authors would like to thank P. Eloy, *Université Catholique de Louvain*, for XPS measurements. A. Aznárez acknowledges financial support from the Public University of Navarra through a PhD fellowship.

Notes and references

- R.M. Heck and R.J. Farrauto, Catalytic Air Pollution Control. Commercial Technology,
 Nostrand Reinhold, New York, 1995.
- 2 M.F.M. Zwinkels, S.G. Jaras, P.G. Menon and T.A. Griffin, *Catal. Rev.-Sci. Eng.*, 1993, **35**, 319.
- 3 R. Prasad, L.A. Kennedy and E. Ruckenstein, Catal. Rev.-Sci. Eng., 1984, 26, 1.
- 4 C.N. Satterfield, *Heterogeneous Catalysis in Industrial Practice*, 2nd Ed. 1991, New York, McGraw-Hill, 1991.
- 5 R. Burch and M.J. Hayes, *J. Mol. Catal. A*, 1995, **100**, 13.
- 6 F. Diehl, J. Barbier-Jr, D. Duprez, I. Guibard and G. Mabilon, *Appl. Catal. B*, 2010, **95**, 217.
- 7 P. Briot, A. Auroux, D. Jones and M. Primet, Appl. Catal., 1990, **59**, 141.
- 8 R.F. Hicks, H.H. Qi, M.L. Young and R.G. Lee, *J. Catal.*, 1990, **122**, 295.
- 9 T.R. Baldwin and R. Burch, *Appl. Catal.*, 1990, **66**, 337.
- 10 K. Sekizawa, M. Machida, K. Eguchi and H. Arai, *J. Catal.*, 1993, **142**, 655.
- 11 A. Gil, S.A. Korili, R. Trujillano and M.A. Vicente, *Pillared Clays and Related Catalysts*, Springer Science: New York, 2010.
- 12 A. Gil, S.A. Korili and M.A. Vicente, *Catal. Rev.-Sci. Eng.*, 2008, **50**, 153.
- 13 A. Gil, R. Trujillano, M.A. Vicente and S.A. Korili, *Ind. & Eng. Chem. Res.*, 2008, 47, 7226.
- 14 A. Aznárez, R. Delaigle, P. Eloy, E.M. Gaigneaux, S.A. Korili and A. Gil, *Catal. Today*, 2015, **246**, 15.
- 15 M.A. Vicente, R. Trujillano, K.J. Ciuffi, E.J. Nassar, S.A. Korili and A. Gil, Pillared Clay Catalysts in Green Oxidation Reactions, in *Pillared Clays and Related Catalysts*, Springer, New York, 2010, pp. 301-318.

- 16 M.R. Schoenberg, J.W. Blieszner and C.G. Papadopoulos, in *Kirk-Othmer Encyclopedia* of *Chemical Technology*, John Wiley & Sons, New York, 1982, p. 228.
- 17 C.F. Murphy and D.T. Allen, *Atm. Environment*, 2005, **39**, 3785.
- 18 A. Aznárez, S.A. Korili and A. Gil, *Appl. Catal. A*, 2014, **474**, 95.
- 19 A. Aznárez, F.C.C. Assis, A. Gil and S.A. Korili, *Catal. Today*, 2011, **176**, 328.
- 20 S.J. Gregg and K.S.W. Sing, Adsorption, Surface Area and Porosity, Academic Press, New York, 1991.
- 21 M.M. Dubinin, Carbon, 1989, 27, 457.
- 22 S. Brouwer, J.C. Groen and L.A.A. Peffer, Stud. Surf. Sci. Catal., 2006, 160, 145.
- 23 S. Barama, C. Dupeyrat-Batiot, M. Capron, E. Bordes-Richard and O. Bakhti-Mohammedi, *Catal. Today*, 2009, **141**, 385.
- 24 G.M. Bancroft, I. Adams, L.L. Coatsworth, C.D. Bennewitz, J.D. Brown and W.D. Westwood, *Anal. Chem.*, 1975, 47, 586.
- 25 J.C. Vedrine, M. Dufaux and C. Naccache, *J. Chem. Soc., Faraday Trans. 1*, 1978, **74**, 440.
- 26 C.D. Wagner, W.M. Riggs, L.E. Davis and J.F. Moulder, in *Handbook of X-ray Photoelectron Spectroscopy*, Eden Prairie: Physical Electronics Division, Perkin-Elmer Corp., Minnesota, 1979.
- 27 L.M.T. Simplicio, S.T. Brandao, E.A. Sales, L. Lietti and F. Bozon-Verduraz, *Appl. Catal. B*, 2006, **63**, 9.
- 28 A.S. Ivanova, E.M. Slavinskaya, R.V. Gulyaev, V.I. Zaikovskii, O.A. Stonkus, I.G. Danilova, L.M. Plyasova, I.A. Polukhina and A.I. Boronin, *Appl. Catal. B*, 2010, **97**, 57.
- 29 K. Otto, L.P. Haack and J.E. Devries, *Appl. Catal. B*, 1992, **1**, 1.
- 30 E. Lesage-Rosenberg, G. Valic, H. Despert, P. Lagarde and E. Freund, *Appl. Catal.*, 1986, **22**, 211.

- 31 J. Goetz, M.A. Volpe, A.M. Sica, C.E. Gigola and R. Touroude, J. Catal., 1995, 153, 86.
- 32 F. Delannay, *Characterization of Heterogeneous Catalysts*, Marcel Dekker Inc., New York, 1984.
- 33 J.L. Benson, H.S. Hwang and M. Boudart, J. Catal., 1973, 30, 146.
- 34 J. Haber, J.H. Block and B. Delmon, *Pure Appl. Chem.*, 1995, **67**, 1257.
- 35 C.H. Bartholomew and R.B. Pannell, *J. Catal.*, 1980, **65**, 390.
- 36 G.J. den Otter and F.M. Dantzenberg, J. Catal., 1978, **53**, 116...
- 37 S. Tauster, Science, 1981, 211, 1121.
- 38 A. Gil, M.A. Vicente and S.A. Korili, *J. Catal.*, 2005, **229**, 119.
- 39 G. Guiu and P. Grange, *J. Catal.*, 1997, **168**, 463.
- 40 G. Chen, W.T. Chou and C.T. Yeh, *Appl. Catal.*, 1983, **8**, 389.
- 41 T. Huizinga, J. Vangrondelle and R. Prins, Appl. Catal., 1984, 10, 199.
- 42 H. Lieske, G. Lietz, H. Spindler and J. Volter, J. Catal., 1983, 81, 8.
- 43 Y.F.Y. Yao, J. Catal., 1984, 87, 152.
- 44 N.W. Cant and W.K. Hall, *J. Catal.*, 1970, **16**, 220.
- 45 A. Baylet, C. Capdeillayre, L. Retailleau, J.L. Valverde, P. Vernoux and A. Giroir-Fendler, *Appl. Catal. B*, 2011, **102**, 180.
- 46 C. Yacou, A. Ayral, A. Giroir-Fendler, A. Baylet and A. Julbe, *Catal. Today*, 2010, **156**, 216.
- 47 H.L. Tidahy, S. Siffert, J.F. Lamonier, R. Cousin, E.A. Zhilinskaya, A. Aboukaïs, B.L. Su, X. Canet, G. De Weireld, M. Frère, J.M. Giraudon and G. Leclercq, *Appl. Catal. B*, 2007, **70**, 377.
- 48 P. Marecot, A. Fakche, B. Kellali, G. Mabilon, M. Prigent and J. Barbier, *Appl. Catal. B*, 1994, **3**, 283.
- 49 H. Shinjoh, H. Muraki and Y. Fujitani, *Appl. Catal.*, 1989, **49**, 195.

- 50 F.H. Ribeiro, A.E. Schach Von Wittenau, C.H. Bartholomew and G.A. Somorjai, *Catal. Rev.-Sci. Eng.*, 1997, **39**, 49.
- 51 R.J. Madon and M. Boudart, *Ind. & Eng. Chem. Fund.*, 1982, **21**, 438.
- 52 A.C. Gluhoi, N. Bogdanchikova and B.E. Nieuwenhuys, J. Catal., 2005, 229, 154.
- 53 Z. Ferhat-Hamida, J. Barbier Jr, S. Labruquere and D. Duprez, *Appl. Catal. B*, 2001, **29**, 195.
- 54 T. Maillet, C. Solleau, J. Barbier-Jr and D. Duprez, Appl. Catal. B, 1997, 14, 85.

Captions

- **Table 1.** Catalyst composition and XPS data.
- **Table 2.** Palladium surface composition (%) of the fresh Pd/Al-PILC catalysts obtained from XPS experiments.
- **Table 3.** Test for heat- and mass-transfer limitations.
- **Table 4.** Kinetic parameters obtained using the Pd/Al-PILC and Pt/Al-PILC catalysts.
- **Scheme 1.** Schematic representation of palladium and platinum particles on the pillared clay structure.
- Figure 1. TPR patterns for the Pd/Al-PILC and Pt/Al-PILC catalysts.
- **Figure 2.** Conversion of propene over the Pd/Al-PILC and Pt/Al-PILC catalysts pre-treated in air.
- **Figure 3.** TPR patterns for the Pd/Al-PILC and Pt/Al-PILC catalysts previously reduced with hydrogen at 300°C for 2 h after use for propene combustion, and freshly prepared.
- **Figure 4.** XRD patterns for the support and catalyst 2Pd (freshly prepared and after use for propene combustion).
- **Figure 5.** Effect of successive oxidation cycles on the catalytic activity of catalysts 0.1Pd and 2Pd for propene combustion. I-III: number of oxidation cycles.

Table 1. Catalyst composition and XPS data.

Catalyst	Binding energies (eV)								Atom ratios			
•	Si 2p Mg 2s		Al 2p	Pd 3d _{5/2}	Pd 3d _{5/2}		Pt 4f _{7/2}		Al/Si	C/Si	Metal/Si	
Al-PILC	102.7	89.1	74.7						0.62	0.52		
0.1Pd	102.9	89.4	74.9	338.1 336.5	335.1				0.62	0.62	0.0021	
0.5Pd	102.9	89.4	74.9	338.1 336.5	335.1				0.61	0.57	0.0325	
1Pd	102.8	89.4	74.8	338.1 336.5	335.1				0.61	0.62	0.0326	
2Pd	102.8	89.3	74.8	338.1 336.5	335.1				0.60	0.63	0.0710	
0.1Pt	102.8	89.4	74.8			73.8	71.7		0.61	0.54	0.0022	
0.5Pt	102.6	89.2	74.7			73.5	71.3		0.58	0.50	0.0039	
1Pt	102.9	89.5	75.0			73.9	71.6		0.59	0.50	0.0049	
2Pt	102.9	89.5	74.9			73.6	71.5		0.59	0.50	0.0073	

Table 2. Palladium surface composition (%) of the fresh Pd/Al-PILC catalysts obtained from XPS experiments.

Catalyst ·	Binding e	Oxidized	Reduced		
	338.1 (Pd ⁿ⁺) (n≥2)	336.5 (Bulk PdO)	335.1 (Pd)	palladium	Palladium
0.1Pd	35	60	5	95	5
0.5Pd	18	74	8	92	8
1Pd	9	71	20	80	20
2Pd	6	70	24	76	24

Table 3. Test for heat- and mass-transfer limitations.

Catalyst		Rate	TOF (1/s) ^a	Propene	D (CO) (%) ^b	Particle size	
		(10 ⁻⁸ mol/s g)	101 (1/8)	conversion (%)	D (CO) (78)	(nm)	
Pt/Al-PILC	0.5% Pt	28	0.059	2.1	19	6.0	
	1.0% Pt	56	0.063	3.5	17.6	6.4	
Pd/Al-PILC	1.0% Pd	131	0.234	8.1	5.6	20	
	2.0% Pd	214	0.250	13.3	4.5	24.9	

Note 1. Pre-treatment of the catalysts in flowing air.

Note 2. Reaction run at 195°C.

^a The number of active sites were counted before reaction by chemisorption of CO at 35°C.

^b Percentage of metal exposed.

Table 4. Kinetic parameters obtained on the Pd/Al-PILC and Pt/Al-PILC catalysts.

]	Pre-trea	atment in flowi		Pre-treatment in flowing hydrogen					
Catalant	dp^a	Metal ^b	E _a c	ln A c	Rate ^d	TOF ^e	C ₃ H ₆	E _a c	ln A c	Rate d	TOF ^e	C ₃ H ₆
Catalyst	(nm) (µ	(µmol/g)	(kJ/mol)	(1/s)	(10 ⁻⁸ mol/s g)	(1/s)	C (%) ^f	(kJ/mol)	(1/s)	(10 ⁻⁸ mol/s g)	(1/s)	C (%) ^f
0.1Pd	3.8	2.2	212.0	51.1	7.4	0.03	0.5	21.8	4.3	69	0.31	4.3
0.5Pd	11.7	4.5	220.8	54.6	49	0.11	3.2	36.1	7.8	117	0.26	7.3
1Pd	20.0	5.6	242.0	60.9	131	0.23	8.1	45.8	10.4	205	0.37	13
2Pd	24.9	8.6	255.2	64.9	214	0.25	13.3	48.9	10.9	241	0.28	15.2
0.1Pt	3.8	1.4	159.0	32.0	0.0	0.00	0	10.3	1.5	56	0.33	3.5
0.5Pt	6.0	4.8	23.9	3.3	28	0.06	2.1	22.9	3.5	45	0.09	2.8
1.0Pt	6.4	8.9	23.7	3.3	56	0.06	3.5	23.4	3.3	63	0.07	3.9
2Pt	8.8	13	23.4	3.0	63	0.05	3.9	23.6	3.0	64	0.05	4

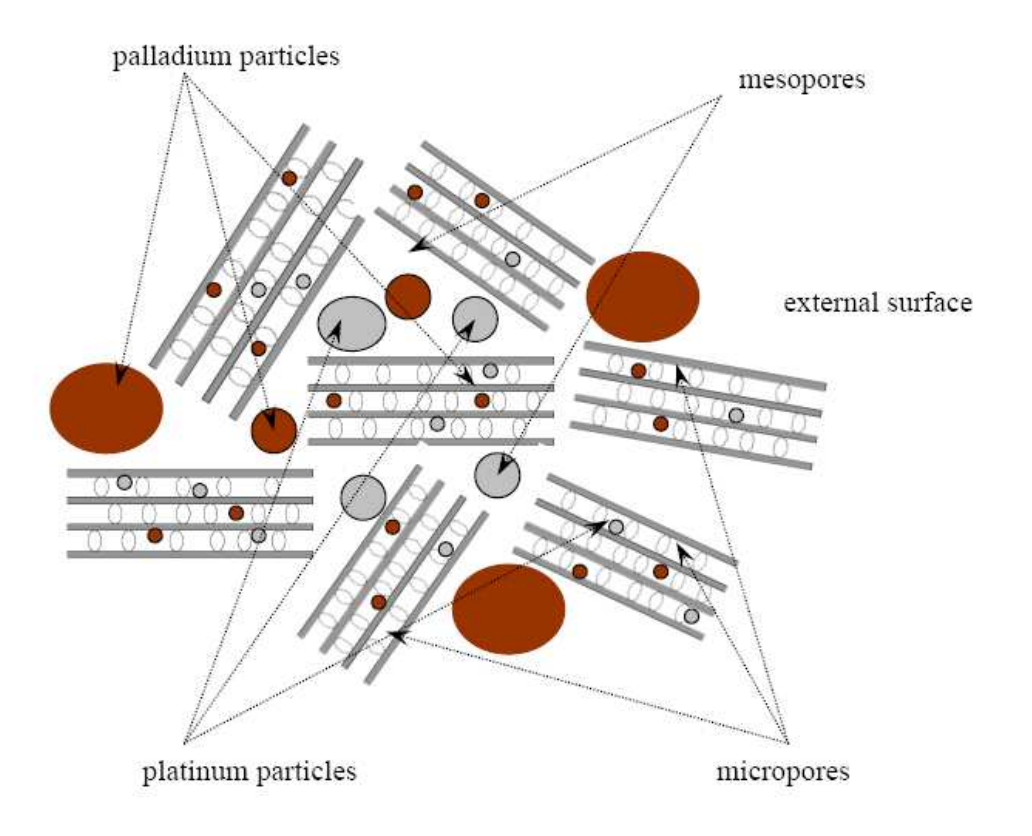
 ^a Mean size of the metal particles, from CO chemisorption at 35°C.
 ^b Number of Pd and Pt surface sites counted by CO chemisorption at 35°C.

^c Determined in the kinetic region.

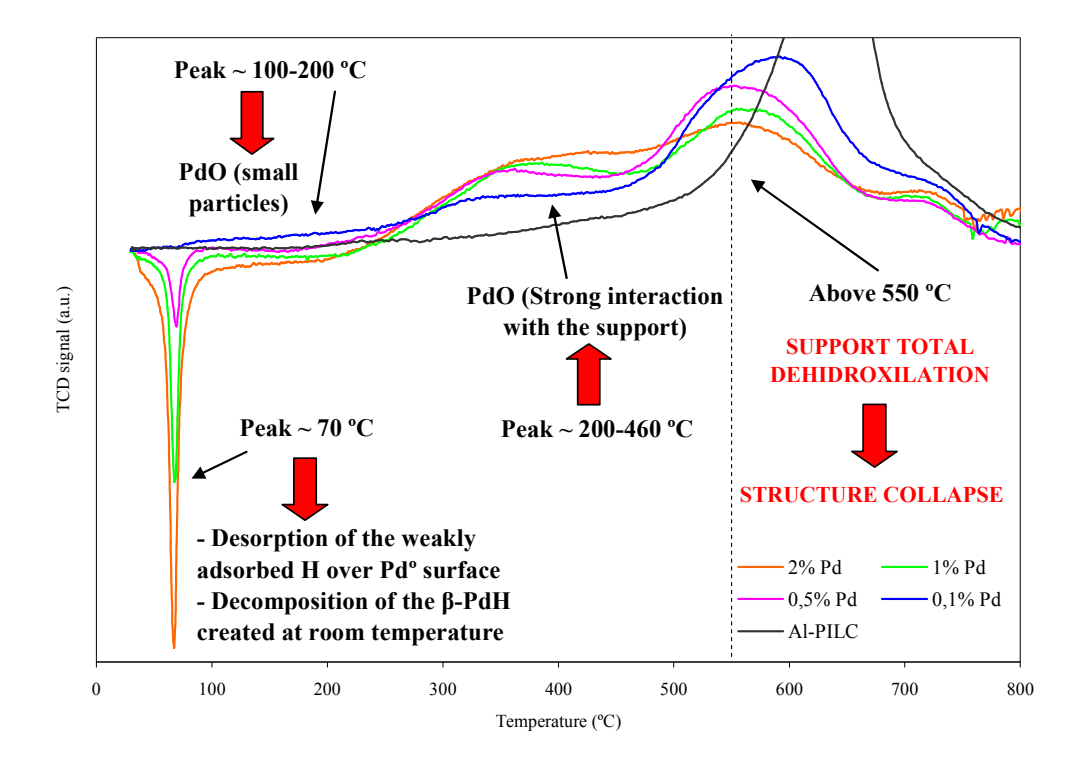
^d Per g of catalyst, at 195°C.

^eRun at 195°C.

^fPercent of propylene converted at steady state at 195°C.



Scheme 1. Schematic representation of palladium and platinum particles on the pillared clay structure.



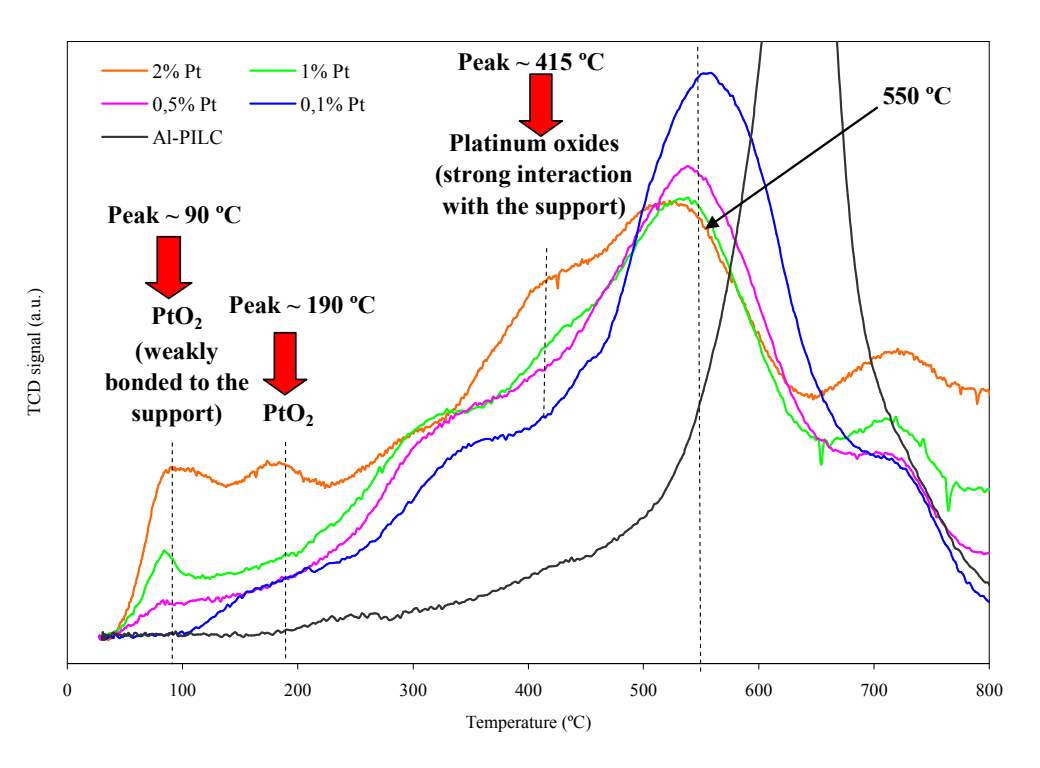


Figure 1. TPR patterns of the Pd/Al-PILC and Pt/Al-PILC catalysts.

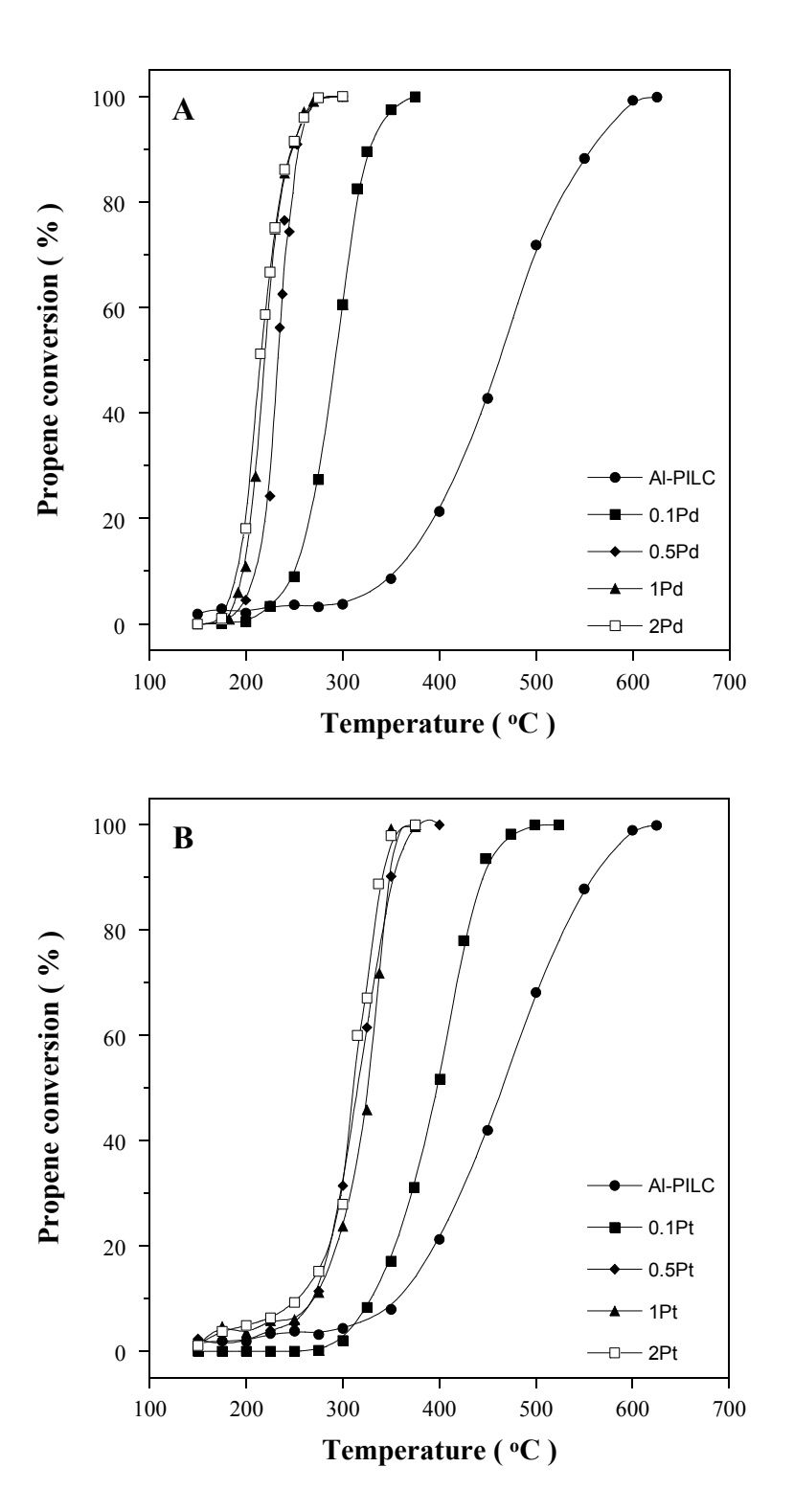
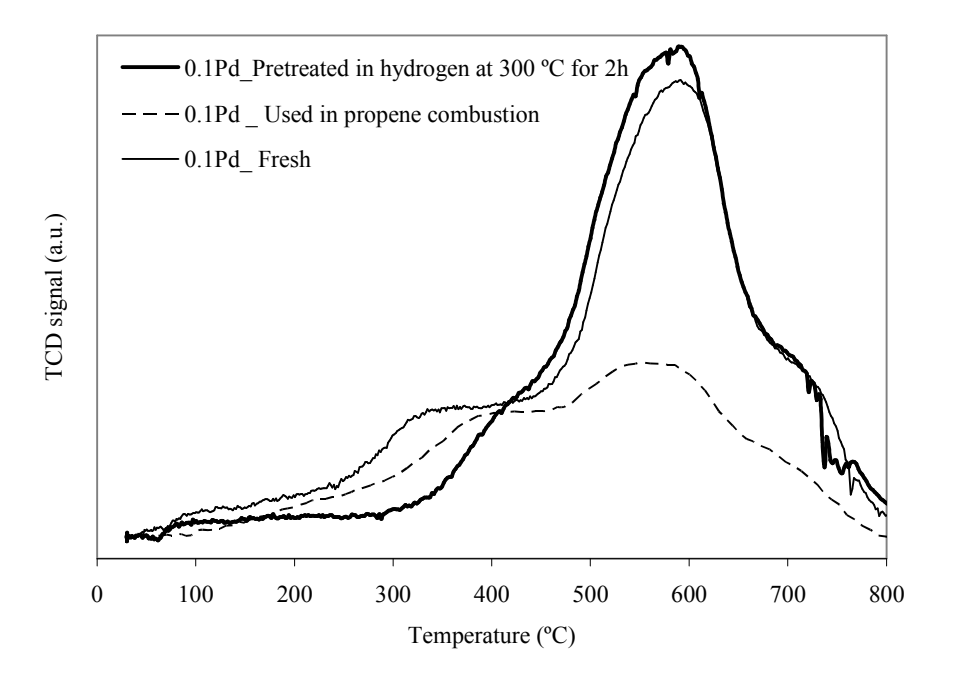


Figure 2. Conversion of propene over the Pd/Al-PILC and Pt/Al-PILC catalysts pre-treated in air.



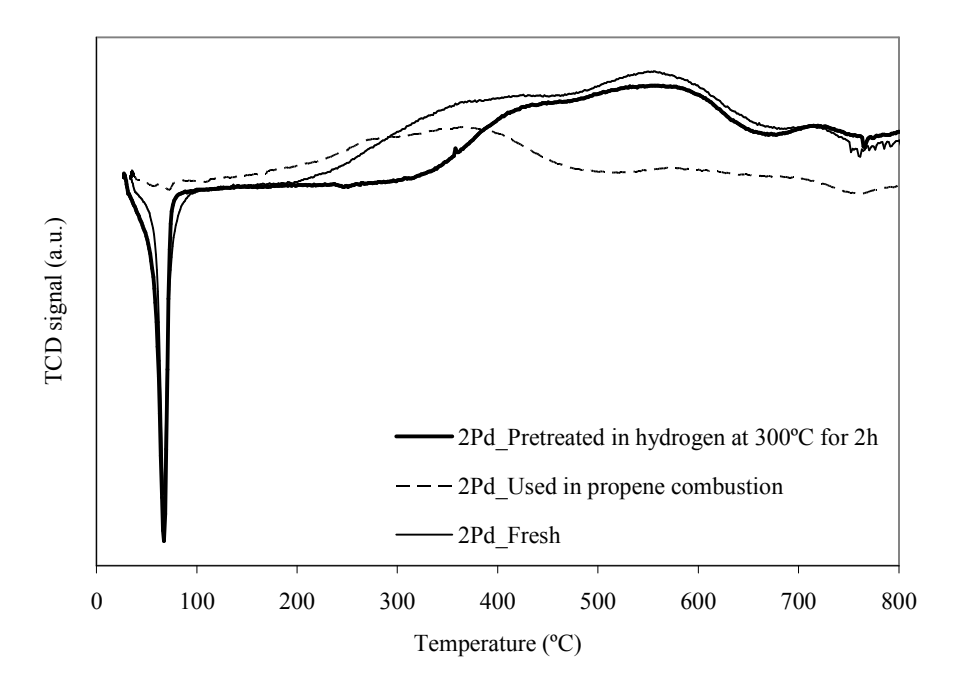


Figure 3. TPR patterns for the Pd/Al-PILC and Pt/Al-PILC catalysts previously reduced with hydrogen at 300°C for 2h, after use for propene combustion, and freshly prepared.

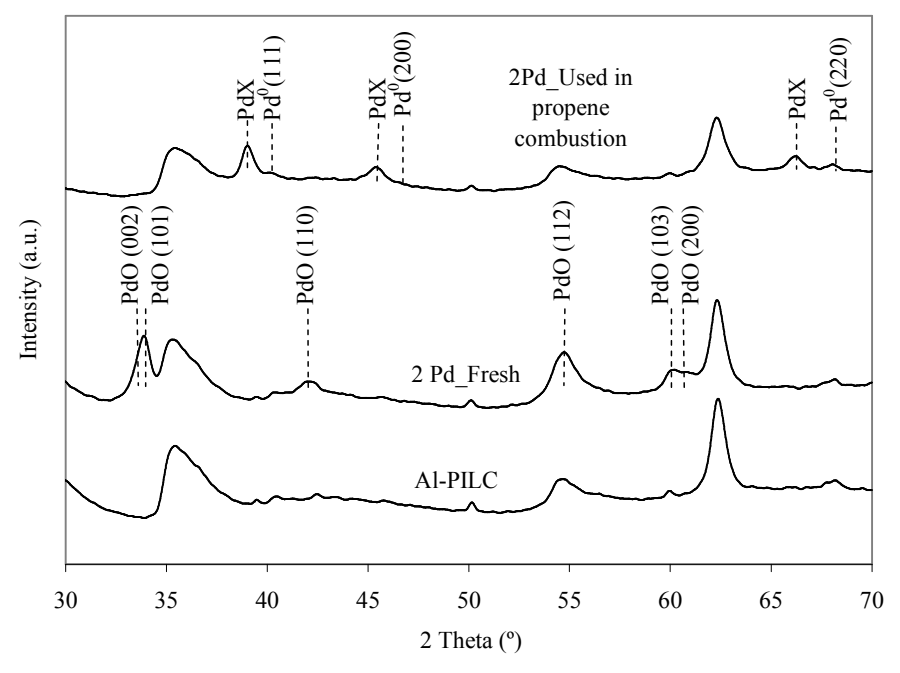


Figure 4. XRD patterns for the support and catalyst 2Pd (freshly prepared and after use for propene combustion).

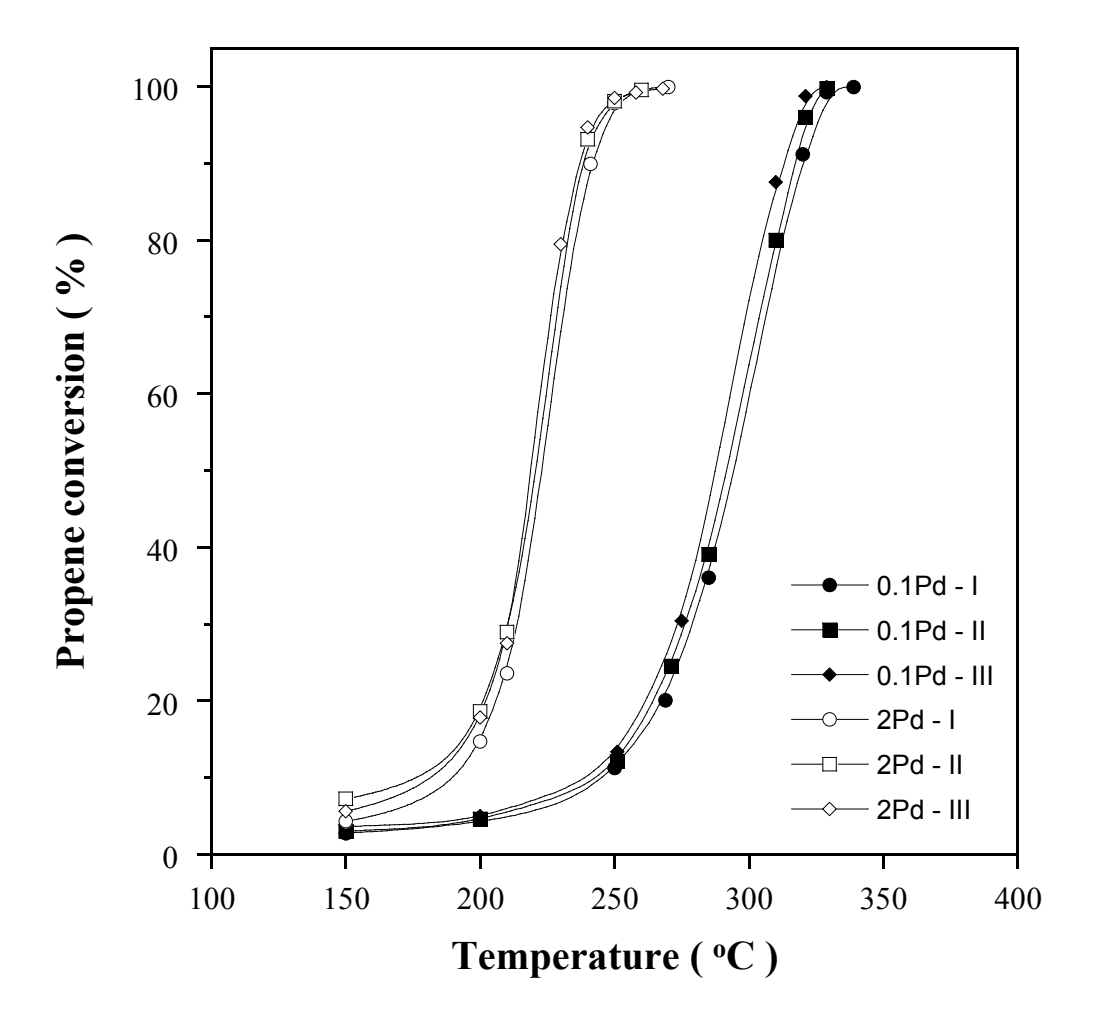


Figure 5. Effect of successive oxidation cycles on the catalytic activity of catalysts 0.1 and 2Pd for propene combustion. I-III: number of oxidation cycles.

Performance of palladium and platinum supported on alumina pillared clays in the catalytic combustion of propene

A. Aznárez, A. Gil*, S.A. Korili

Department of Applied Chemistry, Building Los Acebos, Public University of Navarra, Campus of Arrosadia, E-31006 Pamplona, Spain

